Excitonic effects in the optical spectra of superlattices in an electric field

R. P. Leavitt
U. S. Army Laboratory Command, Harry Diamond Laboratories, 2800 Powder Mill Road, Adelphi, Maryland 20783-1197

J. W. Little
Martin Marietta Laboratories, 1450 South Rolling Road, Baltimore, Maryland 21227

(Received 6 November 1989; revised manuscript received 7 June 1990)

We consider theoretically the optical spectra of electron-hole Stark-ladder transitions in superlattices under an electric field. Electron and heavy-hole subband energies and envelope functions are calculated using a scattering phase-shift treatment of the quasibound, Stark-localized states. Exciton binding energies and oscillator strengths are obtained as functions of the electric field for several pairs of Stark-localized electron and hole states. Accurate and rapid computation of these quantities is achieved by using the simple approximation developed in the preceding paper. We show that observed deviations of the Stark-ladder fan diagram from the expected linear dependence on electric fields result from excitonic effects. We also calculate the absorption coefficient as a function of photon energy for various electric fields, and we compare our results with recent experimental data on short-period GaAs/$Al_xGa_{1-x}As$ superlattices.

I. INTRODUCTION

Although the topic of Stark ladders and electric-field-induced localization of electronic states in solids has been the subject of a long-running theoretical debate,[1] it is only recently that unambiguous confirmation of the predicted phenomena was achieved. The first clear experimental indication of Stark-Wannier localization has been observed in GaAs/$Al_xGa_{1-x}As$ superlattices. Mendez, Agulló-Rueda, and Hong[2] used low-temperature photoluminescence and photocurrent measurements in a superlattice with alternating 30-Å-thick GaAs and 35-Å-thick $Al_{0.35}Ga_{0.65}As$ layers to show the existence of transitions between levels of Stark ladders formed in the valence and conduction bands of the superlattice. Voisin *et al.*[3] studied Stark-ladder transitions in a superlattice with alternating 33-Å-thick GaAs and $Al_{0.3}Ga_{0.7}As$ layers by using low-temperature electroreflectance spectroscopy. By examining these spectra as functions of the electric field (at fixed photon energy), they observed oscillations that were periodic in the inverse of the electric field, as was predicted by Bleuse, Bastard, and Voisin.[4]

Since the publication of the papers cited above, a number of additional experimental studies of the effects of Wannier-Stark localization have appeared in the literature. Agulló-Rueda, Mendes, and Hong[5] have observed a doubly resonant Raman-scattering process, in which both the incident and scattered light are in resonance with electronic transitions involving Stark-localized states in the superlattice. The same authors studied a number of different superlattices, using low-temperature photocurrent spectroscopy.[6] We recently observed Stark-ladder transitions[7] in a strongly coupled superlattice with 19-Å GaAs wells and 17-Å $Al_{0.3}Ga_{0.7}As$ barriers; in this superlattice, the miniband widths are comparable to the valence- and conduction-band offsets. Yan *et al.*[8] investigated the excitons corresponding to the density-of-states singularities at the bottom and top of the minibands (as well as those corresponding to the localized states at high electric fields), using photocurrent spectroscopy, and showed the existence, at room temperature, of an effective blue shift of the excitonic absorption edge, roughly equal to half the sum of the valence and conduction miniband widths. Bar-Joseph *et al.*[9] measured Stark-ladder transitions at room temperature and demonstrated optical bistability resulting from the effective blue shift.

While a large amount of experimental information on the behavior of short-period superlattices has been obtained recently, a detailed theoretical treatment of Wannier-Stark localization in superlattices, including excitonic effects, is lacking. The most comprehensive theoretical treatment to data, that of Bleuse, Bastard, and Voisin,[4] is based almost entirely on the tight-binding approximation and does not consider excitonic effects at all. It is clear, from an examination of the experimental literature on Wannier-Stark localization, that excitons play a major role in the observe phenomena, as they do in corresponding phenomena in isolated quantum wells. For example, large increases in the binding energies for excitons in which electrons and holes are localized in the same well are expected as the character of the excitonic wave function changes from three dimensional to two dimensional with increasing electric field. For this reason, we have undertaken a theoretical study of excitonic effects in short-period superlattices under an electric field. Our treatment is based on the method developed in the preceding paper.[10] The accuracy of this method is comparable to those of other methods that have been developed previously for simple quantum-well structures; furthermore, no other method exists that is sufficiently general to describe the properties of excitons in such complex physical systems. In addition, the Wannier-

Stark-localized superlattice system provides a stringent test for our method.

Our approach yields a form for the binding energy, consisting of an integral (over the electron and hole coordinates perpendicular to the layers) of a prescribed function weighted by the squares of the electron and hole subband envelope functions. In the preceding paper, we showed that the method is capable of rapid and accurate computation of exciton binding energies in quantum-well structures. Therefore, it is reasonable to expect that the method will give good results for more complex physical systems, such as the Stark-localized superlattice considered here. Therefore, the first task of this paper is to calculate the envelope functions themselves (as well as the subband-edge energies). To do this, we use a transfer-matrix method in conjunction with a scattering phase-shift formalism.[11] If the effective masses and the barrier heights in the superlattice are not too small, and if the electric field is not too large, the quasibound resonances representing the subband edges are very sharp (i.e., field-induced tunneling into the continuum is negligible). In this case, a simple boundary condition can be used to obtain the eigenvalue condition, and numerical calculations of the maxima in the density of states[11] are avoided. Furthermore, the resulting envelope functions are normalizable, and the matrix elements required for the rest of the calculations can be obtained without recourse to arbitrary cutoffs. Hence we restrict ourselves to excitons formed from states in the conduction and heavy-hole bands; light-hole states are not considered.

The method described above is only practical for structures with a finite number of layers. Hence, in our calculations, we replace the superlattice of interest with a quantum-well structure containing 11 coupled wells. Specifically, we treat a structure containing 30-Å GaAs quantum wells with 30-Å $Al_{0.35}Ga_{0.65}As$ barriers. This structure is representative of several superlattices that have been studied experimentally.[2,3,5,6,8,9] In Sec. II we present the results of the subband-edge-energy and envelope-function calculations for the truncated 11-well structure. In Sec. III we describe the calculation of exciton binding energies for the structure, and we present the net electron-hole transition energies (including the exciton binding-energy correction) as functions of the electric field. In Sec. IV we discuss the oscillator strengths for electron-hole Stark-ladder transitions; we also show calculations of the optical absorption as a function of incident photon energy for several values of the electric field.

II. CALCULATION OF SUBBAND ENERGIES AND ENVELOPE FUNCTIONS

In our theoretical description of Stark localization in superlattices, we assume that both the valence and conduction bands can be described by parabolic dispersion relations. In so doing, we neglect coupling between conduction and valence bands (which leads to band nonparabolicity[12]) and coupling of the light- and heavy-hole valence bands[13] (which leads to exciton binding-energy corrections[14] on the order of 1–2 meV). Thus subbands within both the valence and conduction bands (at $\mathbf{k}_{\parallel}=0$) are described by single-band envelope functions $f_n^{(j)}$, where $n=1,2,\ldots$ numbers the subbands in order of increasing energy, and $j=e$ or h for electrons and holes.

For a structure with a finite number of layers (with finite barrier heights) in an electric field, there are no true bound states, since there is a nonzero probability of electric-field-induced tunneling into the continuum. However, the envelope functions and subband-edge energies can be calculated by using a scattering phase-shift method[11] to determine the maxima in the density of states associated with the layered structure.

Here, we consider a structure consisting of 11 GaAs wells, 30 Å thick, separated by 30-Å thick $Al_{0.35}Ga_{0.65}As$ barriers, and bounded on either end by semi-infinite layers of $Al_{0.35}Ga_{0.65}As$. Effective-mass parameters (i.e., the conduction-band effective mass m_e and the Luttinger parameters[13] γ_1 and γ_2) for $Al_{0.35}Ga_{0.65}As$ were determined by linear interpolation of the conduction-band masses and the perpendicular hole masses for AlAs (Ref. 15) and GaAs.[15,16] Specifically, we use the following parameters: For GaAs, $m_e=0.067$, $\gamma_1=6.8$, and $\gamma_2=1.9$; for $Al_{0.35}Ga_{0.65}As$, $m_e=0.096$, $\gamma_1=5.49$, and $\gamma_2=1.27$. In terms of the Luttinger parameters, we have $m_{h\parallel}^{-1}=\gamma_1\pm\gamma_2$ and $m_{h\perp}^{-1}=\gamma_1\mp 2\gamma_2$, where the + (−) sign applies for heavy (light) holes. We assume that 70% of the energy-gap discontinuity appears across the conduction band, and therefore we obtain band offsets of 353 and 151 meV for the conduction and valence bands, respectively, where we have used the expression in Ref. 17 for the energy-gap difference between $Al_xGa_{1-x}As$ and GaAs. We consider only electron and heavy-hole states since, in this case, a simple boundary condition (i.e., vanishing of the coefficient of the exponentially growing Airy function in the final barrier) can be used to determine the eigenstates, and the resulting envelope functions are normalizable. The tight-binding approximation described earlier[4] should provide an adequate description of the electronic properties of this structure, since the coupling between adjacent wells is relatively weak.

To aid in interpreting the results of calculations for the superlattice, we also calculated the energy levels for a single 30-Å quantum well as a function of electric field. In this system, the valence-band well supports two bound heavy-hole states. In the conduction band, there is a single bound state, as well as a resonance somewhat above the top of the barrier. The lowest subband-edge energies (relative to the GaAs band edges) calculated for the single well are 150.1 meV for the conduction band and 47.8 meV for the valence band. We calculated also the miniband-edge energies for the lowest miniband of the superlattice at zero electric field by using a Kronig-Penney model, with parabolic bands, using the parameters given above. For the conduction band, we obtained $E_{\min}=131.2$ meV, and $E_{\max}=175.6$ meV. For the valence band, $E_{\min}=44.9$ meV, and $E_{\max}=51.0$ meV. Thus the energies of the miniband centers are 153.4 meV for the conduction band, and 48.0 meV for the valence band; these nearly coincide with the single-well subband-edge energies, as would be expected on the basis of a tight-binding approximation.[4] The miniband widths are

$\Delta_e = 44.4$ meV for the conduction band, and $\Delta_h = 6.1$ meV for the valence band.

For the 11-well system, as many as 22 levels were obtained for each band, with 11 corresponding to the single-well ground states, and the rest corresponding to excited states. Here we consider only those levels associated with the ground levels of the corresponding isolated wells. In Fig. 1 we show the fan diagrams for the (a) electron and (b) heavy-hole Stark ladders. Only levels localized in the five central wells are shown, since the lower and higher levels (i.e., $n = \pm 3$, ± 4, and ± 5) are influenced to some degree by the semi-infinite barriers bounding the structure. The spatial extent of the electron wave function is expected to equal the thickness L of the 11-well structure at a field equal to $\Delta_e / eL = 7$ kV/cm. Thus, for fields well in excess of this value, the boundaries of the 11-well structure should not influence the energies of the central subbands, and the separation of the calculated electron subband energies should follow well the linear behavior expected in an infinite superlattice:[2]

$$E_n(F) = E_{n=0} \mp neFd \ , \tag{1}$$

where F is the electric field, d is the superlattice period (equal to 60 Å), and where the upper (lower) sign holds for electrons (holes). That this is indeed the case can be seen by examining Fig. 1. As expected, the Stark-ladder origins nearly coincide with the single-well energies and the miniband centers for this structure.

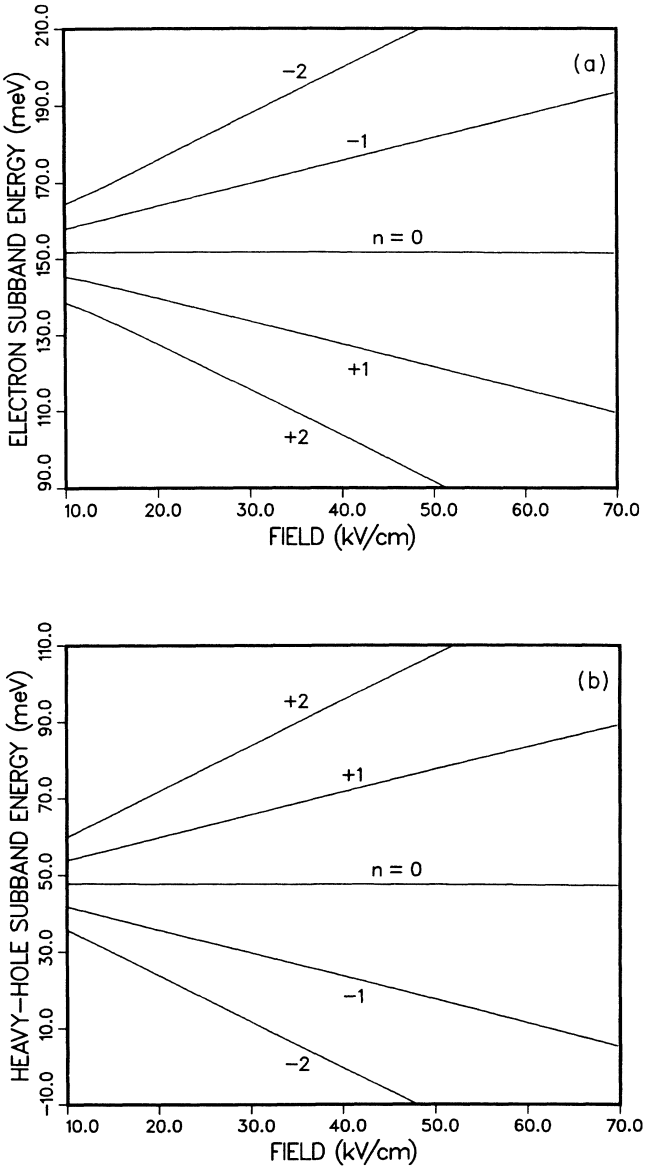

FIG. 1. Calculated (a) electron and (b) heavy-hole subband energies as functions of electric field for a 30-Å/30-Å $GaAs/Al_{0.35}Ga_{0.65}As$ superlattice. The calculation was performed by replacing the superlattice with a coupled quantum-well structure with 11 wells, as described in the text.

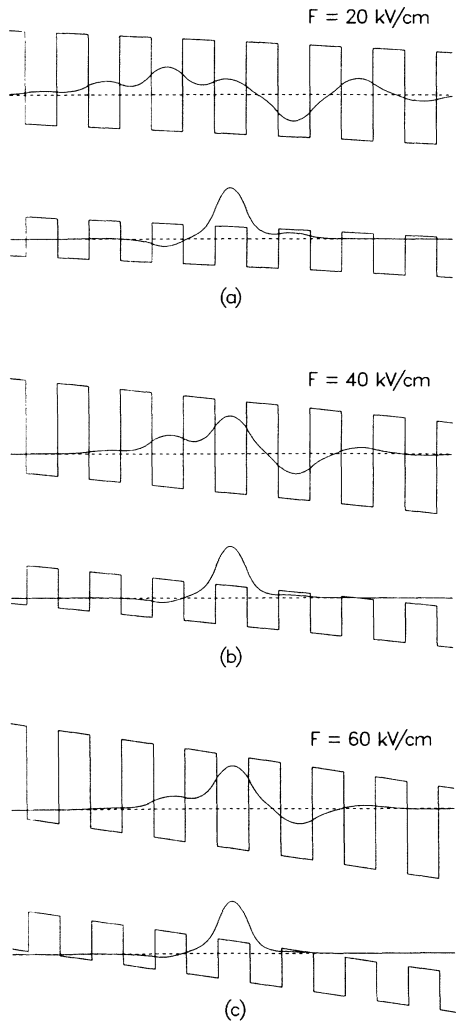

FIG. 2. Electron and hole subband envelope functions for a state localized at the center of the 11-well structure for electric fields of (a) 20, (b) 40, and (c) 60 kV/cm. The valence- and conduction-band profiles are shown also (not to scale). Only the seven central wells of the structure are shown. The horizontal dashed lines show the subband energies; they also serve as zeros for the respective envelope functions.

For fields above 10 kV/cm, the slight deviation of the calculated levels from the simple form of Eq. (1) results from the quantum-confined Stark effect[18] in the isolated well (i.e., $E_{n=0}$ acquires a dependence on F). This was confirmed by comparing the energies of the 11-well central level ($n=0$) with those obtained in the single-well calculation. Identical Stark shifts were obtained, both in the valence and in the conduction bands. For a 30-Å well, a total shift (electron plus hole) of only 0.78 meV is obtained for a field of 70 kV/cm.

In Fig. 2 we show the electron and hole subband envelope functions for electric fields of 20, 40, and 60 kV/cm. Also shown is a schematic energy-band diagram for the seven central wells of the 11-well structure for each electric field. As the magnitude of the electric field increases, the spatial extent of the electron and hole subband envelope functions decreases. At 20 kV/cm, the hole envelope function is nearly localized to a single well, whereas the electron envelope function extends over about five wells. At 40 kV/cm, the electron envelope function extends over three wells, and at 60 kV/cm it is mostly localized in the central well. Note that each envelope function has at least one node within the seven-well region shown (even though it corresponds to the single-well ground state). This alternation in sign of the envelope function is necessary to preserve orthogonality of envelope functions centered on adjacent wells, and is important in determining the oscillator strengths for electron-hole transitions, as we will discuss later in this paper.

III. EXCITON BINDING ENERGIES

In the preceding paper,[10] we developed a simple method for calculating exciton binding energies in quantum-confined structures. Here, we apply the method to calculate exciton binding energies in superlattices in an electric field.

It is convenient to express the results of Ref. 10 in terms of the electron-hole correlation function, defined by

$$C_{nm}(Z)=\int_{-\infty}^{\infty} dz\,|f_n^{(e)}(z+Z)|^2|f_m^{(h)}(z)|^2\ , \tag{2}$$

where $f_n^{(e)}$ and $f_m^{(h)}$ are the envelope functions for electron subband n and hole subband m, respectively. We may write the binding energy of the exciton associated with the pair (n,m) of subbands as follows:

$$E_{nm}^B=E_0\int_{-\infty}^{\infty} dZ\ C_{nm}(Z)w(Z/a_0)\ , \tag{3}$$

where $E_0=\mu_{nm}e^4/2\epsilon^2\hbar^2$, $a_0=\epsilon\hbar^2/\mu_{nm}e^2$, ϵ is the dielectric constant of the structure, and $w(Z/a_0)$ is the (normalized) binding energy for a system in which the electron and hole are confined to two planes separated by a distance Z, as given in Ref. 10. The density-of-states reduced mass, μ_{nm}, is given by

$$(\mu_{nm})^{-1}=\int_{-\infty}^{\infty} dz\,|f_n^{(e)}(z)|^2/m_e(z) + \int_{-\infty}^{\infty} dz\,|f_m^{(h)}(z)|^2/m_{h\parallel}(z)\ . \tag{4}$$

Exciton binding energies were calculated for the 11-well structure as functions of electric field using Eq. (3). In performing this calculation, we selected pairs of states (n,m) for which the presence of the boundaries (i.e., the semi-infinite $Al_{0.35}Ga_{0.65}As$ layers bounding the 11 wells) had negligible influence. Generally, we chose pairs of states close to the center of the structure for calculating the binding energies for states in which the electron is centered in well n and the hole is centered in well $n+p$, which we label as $CB(n)\rightarrow hh(n+p)$. We verified that the boundaries of the 11-well structure did not influence the binding-energy results by comparing calculated binding energies for $CB(n)\rightarrow hh(n+p)$ and $CB(n\pm1)\rightarrow hh(n+p\pm1)$; these values agreed to better than 0.02 meV.

In Fig. 3, we show the results of the exciton binding-energy calculation. For the $p=0$ (i.e., spatially direct) transition, the binding energy increases monotonically with increasing electric field above 10 kV/cm. This is expected since, as the electron and hole subband envelope functions become increasingly localized, the increasing Coulomb attraction leads to a lowering of the total energy, and thus to an increase in the binding energy of the exciton. At 70 kV/cm, the binding energy, 9.5 meV, is somewhat below the value of 10.1 meV calculated for an isolated 30-Å well, but is expected to approach the latter value as the wave function becomes fully confined (with increasing electric field) to a single well.

The exciton binding energies for the spatially oblique transitions (i.e., $p\neq0$) show qualitatively different behavior. As the field increases, the binding energies initially increase, go through a maximum, and then finally decrease to a constant value corresponding to electrons and holes localized in planes separated by $|p|d$. The field at which the maximum occurs depends on p and is lower for larger $|p|$. This can be easily understood in terms of Eq. (3). The maximum in the binding energy for a given exci-

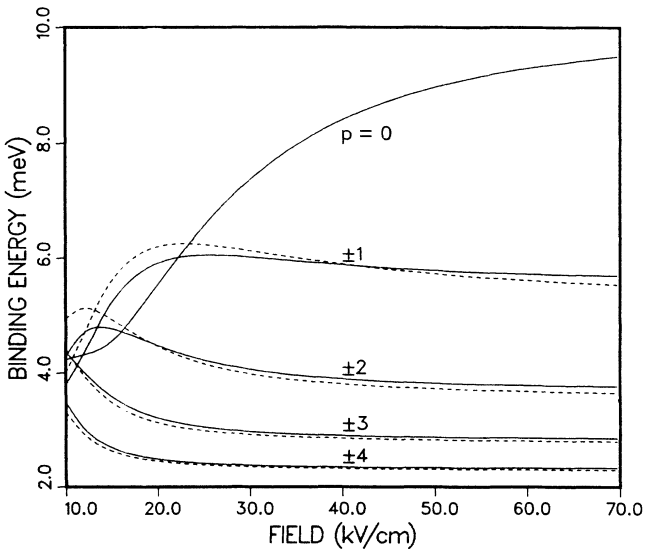

FIG. 3. Calculated binding energies for the $CB(n)\rightarrow hh(n+p)$ Stark-ladder excitons as functions of electric field in a 30-Å/30-Å $GaAs/Al_{0.35}Ga_{0.65}As$ superlattice. Binding energies for $p<0$ are shown as dashed lines for clarity.

ton occurs roughly when the probability of finding an electron and a hole in the same well is highest, since $w(Z/a_0)$ is strongly peaked around $Z=0$. Since the hole subbands are nearly localized in a single well for the fields under consideration, the maximum of Eq. (3) for a given pair of states occurs at an electric field for which the probability of an electron being $|p|$ wells away from its center position is greatest. At very low fields, the electron state extends over many wells, and the probability of finding the electron p wells away is very small. At high fields, the electron is confined in a single well, and this probability is again small. For some intermediate value of the field, where the electron state extends over a few wells, there should be an enhanced probability of finding the electron $|p|$ wells away from its center position. The maximum probability obviously occurs at lower fields for larger $|p|$, since the spatial extent of the wave function is inversely proportional to the field.

In Fig. 4 we present the calculated electron-hole transition energies for the 11-well structure, including the exciton binding-energy correction. In contrast to the electron and hole subband-edge energies, there are significant deviations from linear behavior as a function of electric field. These results are in close agreement with the experimental results presented by Mendez, Agulló-Rueda, and Hong (in Ref. 2), who pointed out, specifically, the deviation from linearity in the experimental results for $p=0$. Our calculations show that this deviation is entirely due to the dependence of the exciton binding energy on the electric field. Also, the $p=-1$ transition deviates somewhat from linearity, although the deviation is not as strong as that reported in Ref. 2. However, in a later paper,[6] the same authors show a strictly linear dependence on field of the $p=-1$ transition in a similar superlattice.

IV. OSCILLATOR STRENGTHS AND ABSORPTION SPECTRA

Given the electron and hole subband envelope functions, we can calculate the oscillator strengths for band-to-band and excitonic transitions by determining the envelope-function overlap integral:

$$I_{nm}=\int_{-\infty}^{\infty} dz\, f_n^{(e)}(z) f_m^{(h)}(z)\ . \tag{5}$$

The oscillator strength for the band-to-band transitions is proportional to the square of I_{nm}. In the approach of the preceding paper[10] used in calculating excitonic properties, the oscillator strength for excitonic transitions also contains the factor $|g(\rho=0;z=0)|^2$, which is inversely proportional to the effective Bohr radius a_0. This latter factor depends on details of the structure, electric fields, etc., only through the quantities ϵ and μ_{nm}. Our subband-level calculations (see Sec. II) show that μ_{nm} is essentially independent of the electric field. Therefore we may take the band-to-band and excitonic oscillator strengths as being strictly proportional.

In Fig. 5 we show the quantity $I^2_{n,n+p}$ as a function of electric field for the Stark-ladder transitions, with $p=0$, ±1, ±2, and ±3. The behavior of the oscillator strengths for these transitions as functions of electric field mimics that of the exciton binding energies in several respects. First, the oscillator strength for the spatially direct ($p=0$) transitions increases monotonically with increasing electric fields above 17.5 kV/cm. This result is easily understood in terms of the increasing localization of the electron subband envelope function, and the corresponding increase in its overlap with the localized hole envelope function with increasing field. At about 17.5 kV/cm, the oscillator strength has a zero, which results

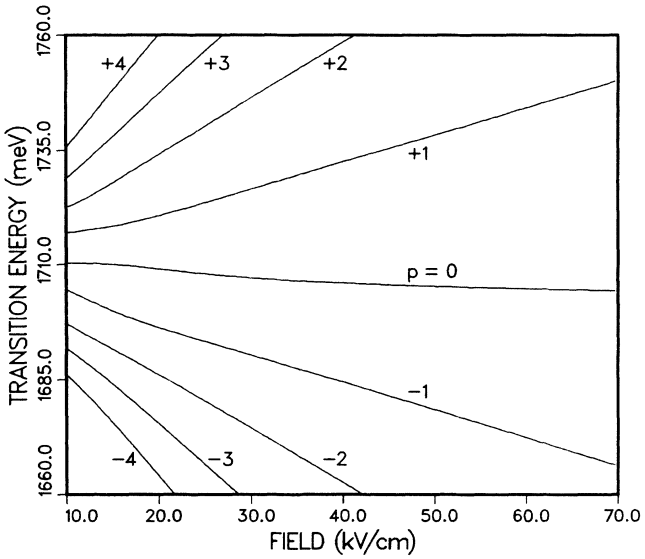

FIG. 4. Calculated transition energies (including exciton binding-energy corrections) for the $CB(n)\rightarrow hh(n+p)$ Stark-ladder transitions as functions of electric field in a 30-Å/30-Å $GaAs/Al_{0.35}Ga_{0.65}As$ superlattice.

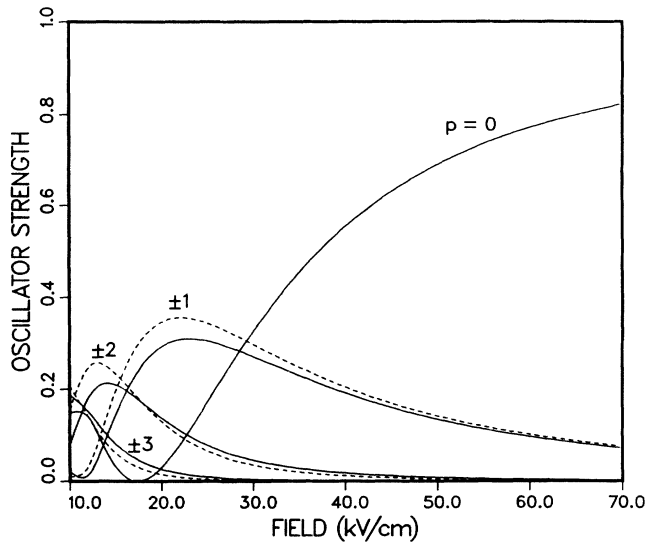

FIG. 5. Calculated oscillator strengths for the $CB(n)\rightarrow hh(n+p)$ Stark-ladder transitions as functions of electric field in a 30-Å/30-Å $GaAs/Al_{0.35}Ga_{0.65}As$ superlattice. Oscillator strengths for $p<0$ are shown as dashed lines for clarity.

from a cancellation within the overlap integral arising from the alternating signs of the electron and hole subband envelope functions (see Sec. II).

For the spatially oblique transitions ($p \neq 0$), there is a maximum in the oscillator strength at a finite value of the electric field, corresponding roughly to the field at which the exciton binding energy is a maximum. These results are in good agreement with the tight-binding results,[4] in which

$$I^2_{n,n+p} = J^2_p((\Delta_e + \Delta_h)/2eFd) \tag{6}$$

where J_p is the pth-order Bessel function. In particular, the calculated maxima in the oscillator strengths agree well with those predicted by Eq. (6). (Deviations are most significant in the region below 10 kV/cm, not shown, where boundary effects become important.) Note, however, that the tight-binding result is independent of the sign of p, whereas our result, based on the envelope-function approximation, is not.

Using our results for the electron and hole subband energies, exciton binding energies, and oscillator strengths, we calculated the absorption as a function of photon energy for several values of the electric field. In the calculation, we represented the absorption for each transition as a sum of excitonic and band-to-band contributions. The band-to-band contribution should contain a factor accounting for the Coulomb attraction in the continuum radial envelope function, which, for a purely two-dimensional electron-hole system, is given by the two-dimensional Sommerfeld factor.[19] However, our calculations on simple quantum-well systems show that this factor is actually much smaller than that for a purely two-dimensional system, and is, in fact, close to unity for all energies. Thus we neglect this factor here, and we write the absorption as follows:

$$\alpha_{nm} = I^2_{nm}\left[\frac{r}{\pi\delta}\exp\left[-\frac{(\hbar\omega - E^{\rm ex}_{nm})^2}{\delta^2}\right] + \tfrac{1}{2}\mathrm{erf}\left[\frac{\hbar\omega - E^{\rm bb}_{nm}}{\delta}\right] + \tfrac{1}{2}\right], \tag{7}$$

where $E^{\rm bb}_{nm} = E_g + E^{(e)}_n + E^{(h)}_m$, $E^{\rm ex}_{nm} = E^{\rm bb}_{nm} - E^B_{nm}$, r is a parameter describing the relative strengths of excitonic and band-to-band transitions, δ is a broadening parameter, and erf(x) is the error function.[20] We chose a Gaussian form for the line shape, since, for this small well width, the broadening mechanism is primarily inhomogeneous (associated with well-width fluctuations).

Representative absorption spectra are shown in Fig. 6, where we have chosen $r = 25$ meV and a full width at half maximum of 12 meV for the exciton line-shape function. (These parameters were chosen to give good agreement of the calculated spectrum with the high-field experimental results of Ref. 2.) Our results are qualitatively very similar to those reported in Refs. 2 and 6. Note, particularly, the existence of a field regime (between 10 and 25 kV/cm, in our case) where the $p = 0$ transition is very weak. This result has been confirmed experimentally in low-temperature studies by Agulló-Rueda, Mendez, and Hong[6] in a superlattice with $L_w = 40$ Å, and $L_b = 20$ Å, in the 15–20 kV/cm range.

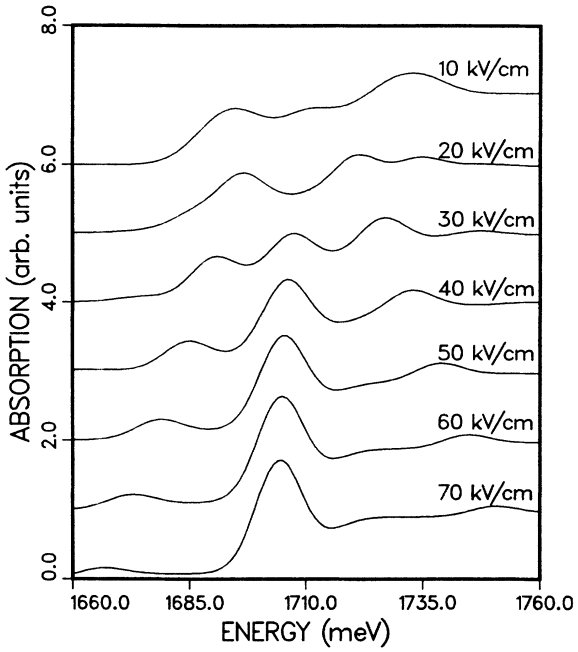

FIG. 6. Simulated absorption spectra corresponding to $CB(n) \rightarrow \mathrm{hh}(n+p)$ Stark-ladder transitions as functions of energy in a 30-Å/30-Å $GaAs/Al_{0.35}Ga_{0.65}As$ superlattice for electric fields between 10 and 70 kV/cm.

V. DISCUSSION AND CONCLUSIONS

We have calculated quantities related to the optical spectra of superlattices in an electric field. Specifically, we considered a $GaAs/Al_{0.35}Ga_{0.65}As$ superlattice with 30-Å thicknesses for both well and barrier layers. By truncating this superlattice to a coupled-quantum-well structure with 11 wells, we were able to use a transfer-matrix method in conjunction with a scattering phase-shift determination of the quasibound electron and hole subband energies and envelope functions. For electric fields in excess of 10 kV/cm, this finite-well representation provided an accurate description of the Wannier-Stark–localized electron and heavy-hole states. Effects associated with the edges of the truncated structure were shown to be negligible in this electric-field regime. Whereas the heavy-hole envelope functions were essentially localized to a single well for fields larger than a few kV/cm, fields considerably larger than 70 kV/cm were needed to fully localize the electron subband envelope functions.

Exciton binding energies were calculated as functions of electric field by using the method developed in the preceding paper.[10] In this approach, the exciton binding energy is given as the integral over the z coordinates of a prescribed function, the binding energy for an exciton formed from an electron-hole pair confined to spatially separated planes, weighted by the probability density for a given electron-hole-pair separation, i.e., the electron-hole correlation function. Calculations of the binding en-

ergies for an exciton formed with an electron centered in well n and the hole centered in well $n+p$ gave results that are consistent with experimental data. Specifically, the binding energy for the spatially direct ($p=0$) exciton approaches that of a single, isolated well of the same width as the field becomes large and localization to a single well becomes complete. In contrast, the binding energy for an oblique ($p\neq 0$) exciton has a maximum at a finite value of the electric field, corresponding roughly to a maximum in the probability of finding the electron and hole separated by $|p|$ wells. Our results show that deviations from simple linear behavior in the measured energies of optical transitions between levels of the Stark ladders, reported in Ref. 2, are entirely due to excitonic effects.

We also calculated the oscillator strengths for band-to-band and excitonic transitions. In our approach, the excitonic oscillator strength for a given transition $CB(n)\rightarrow \mathrm{hh}(n+p)$ is strictly proportional to the band-to-band oscillator strength. The oscillator strength for the $p=0$ transition approaches that for the single, isolated well as the field becomes large. On the other hand, the oscillator strength for a $p\neq 0$ transition has a maximum at a finite value of the electric field. These results are in good agreement with tight-binding calculations,[4] although our results are not symmetric with respect to the sign of p, whereas the tight-binding result is. Given the subband energies, exciton binding energies, and oscillator strengths, we were able to calculate the absorption spectra for the 11-well system as functions of photon energy for various electric fields. Our results are in qualitative accord with experimental low-temperature photocurrent spectra measured in similar superlattices.[2,6]

The Stark-localized superlattice has provided a stringent test of our method for calculating exciton binding energies in quantum-confined structures. As in Ref. 10, the most serious drawback of the method is its neglect of valence-band coupling by off-diagonal terms in the Luttinger Hamiltonian.[13] In the case of isolated quantum wells, inclusion of these terms leads to positive corrections to the binding energies on the order of 1–2 meV. We may safely assume that this is the case for the binding energies of the Stark-localized excitons as well. Furthermore, our result for the excitonic oscillator strengths does not allow for the possible contraction of the exciton in the radial direction with increasing localization of the electron and hole states. Thus the strict proportionality of excitonic and band-to-band oscillator strengths may not hold in real physical systems. This limitation, and the neglect of a Sommerfeld-type factor in the expression for the band-to-band optical absorption, has prevented quantitative agreement of our calculated absorption curves with experiment. Nonetheless, all the features reported experimentally have been qualitatively reproduced here.

In conclusion, we have performed calculations of the electron and hole subband energies and envelope functions, exciton binding energies, and oscillator strengths in a $GaAs/Al_{0.35}Ga_{0.65}As$ superlattice (with layer thicknesses of 30 Å for both well and barrier materials) as functions of electric field. Our results have explained several phenomena observed experimentally in Wannier-Stark–localized systems. We have also shown the practical utility of our approach for performing rapid and accurate calculations of exciton binding energies in complex, quantum-confined semiconductor systems.

[1]See, for example, G. H. Wannier, Phys. Rev. **117**, 432 (1960); J. Zak, Phys. Rev. Lett. **20**, 1477 (1968); G. H. Wannier, Phys. Rev. **181**, 1364 (1969); J. Zak, *ibid.* **181**, 1366 (1969); A. Rabinovitch and J. Zak, Phys. Lett. **40A**, 189 (1972); J. N. Churchill and F. E. Holstrum, *ibid.* **85A**, 453 (1981).

[2]E. E. Mendez, F. Agulló-Rueda, and J. M. Hong, Phys. Rev. Lett. **60**, 2426 (1988).

[3]P. Voisin, J. Bleuse, C. Bouche, S. Gaillard, C. Alibert, and A. Regreny, Phys. Rev. Lett. **61**, 1639 (1988).

[4]J. Bleuse, G. Bastard, and P. Voisin, Phys. Rev. Lett. **60**, 220 (1988).

[5]F. Agulló-Rueda, E. E. Mendez, and J. M. Hong, Phys. Rev. B **38**, 12 720 (1988).

[6]F. Agulló-Rueda, E. E. Mendez, and J. M. Hong, Phys. Rev. B **40**, 1357 (1989).

[7]R. P. Leavitt and J. W. Little, Phys. Rev. B **41**, 5174 (1990).

[8]R. H. Yan, R. J. Simes, H. Ribot, L. A. Coldren, and A. C. Gossard, Appl. Phys. Lett. **54**, 1549 (1989).

[9]I. Bar-Joseph, K. W. Goossen, J. M. Kuo, R. F. Kopf, D. A. B. Miller, and D. S. Chemla, Appl. Phys. Lett. **55**, 340 (1989).

[10]R. P. Leavitt and J. W. Little, preceding paper, Phys. Rev. B **42**, 11 774 (1990).

[11]E. J. Austin and M. Jaros, Phys. Rev. B **31**, 5569 (1985).

[12]K. H. Yoo, L. R. Ram-Mohan, and D. F. Nelson, Phys. Rev. B **39**, 12 808 (1989).

[13]J. M. Luttinger and W. Kohn, Phys. Rev. **97**, 869 (1955).

[14]G. D. Sanders and Y.-C. Chang, Phys. Rev. B **32**, 5517 (1985).

[15]P. Lawaetz, Phys. Rev. B **4**, 3460 (1971); H. C. Casey, Jr., and M. B. Panish, *Heterostructure Lasers, Part B: Materials and Operating Characteristics* (Academic, New York, 1978).

[16]B. V. Shanabrook, O. J. Glembocki, D. A. Broido, and W. I. Wang, Phys. Rev. B **39**, 3411 (1989).

[17]D. Huang, G. Ji, U. K. Reddy, H. Morkoc, F. Xiong, and T. A. Tombrello, J. Appl. Phys. **63**, 5447 (1988).

[18]D. A. B. Miller, D. S. Chemla, T. C. Damen, A. C. Gossard, W. Wiegmann, T. Wood, and C. A. Burrus, Phys. Rev. B **32**, 1043 (1985).

[19]M. Shinada and S. Sugano, J. Phys. Soc. Jpn. **21**, 1936 (1966).

[20]W. Gautschi, in *Handbook of Mathematical Functions,* Natl. Bur. Stand. Appl. Math. Ser. No. 55, edited by M. Abramowitz and I. Stegun (U.S. GPO, Washington, D.C., 1964), p. 297.